PCCP

A directly linked pyrene–dimethylaniline derivative as a potential biochemical sensor for the microenvironmental dielectric properties of the active site of enzymes†

Angela S. F. Ramos and Simone Techert

Max-Planck-Institut für biophysikalische Chemie, Abteilung Spektroskopie und Photochemische Kinetik, Am Fassberg 11, 37077, Göttingen, Germany. E-mail: stecher@gwdg.de

Received 2nd July 2003, Accepted 16th September 2003
First published as an Advance Article on the web 2nd October 2003

Permittivity is a very important physical parameter for a detailed understanding of interactions in a biological system. However, at the moment no common experimental method is available for measuring the dielectric constants of a microenvironment or on a local level, and one has to rely on theoretical simulations. In this work we can demonstrate that it is experimentally possible to estimate the dielectric constant of the active site of the enzyme acetylcholinesterase, based on the spectroscopic properties of the laser dye *N*,*N*-dimethyl(4-pyren-1-ylphenyl)amine. It was found that the dye specifically attaches to the active site of acetylcholinesterase and therefore inhibits its functionality. The microenvironmental dielectric properties, which are spectroscopically sensed, and enzymatic functionality can be combined and might potentially be developed to a biosensing element.

Introduction

Sensors in the biomedical or chemical field can be defined broadly as devices that detect specific molecules or biological processes and convert this information into a signal. In recent years considerable effort has been undertaken to optimize such sensing devices by optimizing the used sensing technique, by miniaturization processes[1–4] or by expanding their area of activity including new biochemical sensor systems.[5–7]

In this work, we introduce a target system, which spectroscopically monitors the dielectric properties of a microenvironment of a protein and might therefore potentially be used in the development of biosensors. The biological role of a protein, and therefore its role in the complexity of cellular action and recognition depends highly on the interaction with other biomolecules. The specificity and efficiency of these interactions are determined through van der Waals forces, hydrogen bonding and electrostatic interactions. The latter are determined by Coulomb interactions, which are a function of the dielectric constant. Changes in the dielectric constant influence the extent of binding between ligand and biomolecules and can even affect the reaction pathway.

Normally, biochemical reactions are investigated in aqueous solutions. Consequently, the dielectric constant of water is used for the description of these reactions. Very often, however, the dielectric properties of the specific protein binding site differ from those of water due to the characteristics of the (apolar and/or aromatic) residues which form the binding sites in the protein.

By choosing an appropriate molecular system as a target molecule, we can demonstrate that it is possible to link directly and in a unique way biological activity and functionality of a system with the spectroscopic features of the chemical target. As spectroscopic sensor system we used the laser dye *N*,*N*-dimethyl(4-pyren-1-ylphenyl)amine (PyDMA), a substance that can probe the microenvironmental properties of the protein binding site. As a model protein the enzyme acetylcholinesterase (AChE) was chosen. Also other proteins or enzymes might be considered, as long as the protein provides a similar substrate specificity as AChE and PyDMA (steric and chemical interaction possibilities with the active site). AChE is an enzyme that hydrolyses the neurotransmitter acetylcholine in the synaptic cleft. The active site is in the bottom of a narrow gorge, which has 14 aromatic residues (Fig. 6(a)). The amine group of the acetylcholine interacts with the anionic subsite,[8] and the acetate group binds to the esteratic subsite.[9]

Because of the pivotal role of acetylcholinesterase in the nervous system, the enzyme has long been an attractive target for the rational design of mechanism-based inhibitors. For example, carbamates, physostigmine and neostigmine are useful therapeutic agents in the treatment of glaucoma and *myasthenia gravis*, respectively.[10] The inhibitor tacrine is widely used against Alzheimer's disease.[11] In order to predict correctly the properties of biomolecular systems, a detailed description of the enzyme is required, including parameters such as the local dielectric constant of the active site. However, an actual problem of rational design is, that in most cases the local dielectric constant or the dielectric constant of the active site in the microenvironment is unknown and has to be assumed theoretically from continuum models or MD simulations.[12]

In this work we can show that, because of the spectroscopic characteristics of PyDMA, information on the microenvironmental dielectric properties of AChE (local permittivity) can be given. On the other hand, based on the analysis of AChE enzyme kinetics according to the Michaelis–Menten model, we elucidated the influence of the PyDMA molecule on the activity of AChE and found a competitive inhibition of the enzyme-supported hydrolysis. Therefore it is possible to combine spectroscopic signalling of the laser dye with the enzyme activity in order to characterize the local permittivity of the active site.

† Presented at the annual meeting of the Deutsche Bunsen-Gesellschaft für Physikalische Chemie, Kiel, Germany, May 29–31, 2003.

 DOI: 10.1039/b307551f

Experimental section

Materials

Achetylcholinesterase type V-S from *Electrophorus electricus* was purchased from Sigma, purified as described previously,[13] concentrated in Vivaspin concentrator, membrane 10 000 MWCO (Vivascience) and stored in 4 mM potassium phosphate buffer, pH 8.0 at $T = -20\,^{\circ}C$. The used solvents were purchased from Merck (spectroscopic grade): acetylacetone, acetonitrile, benzene, chlorobenzene, chloroform, dichloroethane, diethylene glycol, diethyl ether, dimethylethane, dimethylformamide, DMSO, ethyl acetate, ethylene glycol, ethanol, formamide, 1-hexanol, 3-hexanol, methanol, *n*-heptane, *n*-hexane, 1-pentanol, 1-propanol, tetrahydrofuran, toluene. *N*,*N*-Dimethyl(4-pyren-1-ylphenyl)amine (PyDMA) was prepared as described earlier.[14] 5-5′-Dithio-bis(2-nitrobenzoic acid) (DTNB) was purchased from Sigma.

Methods

Enzymatic assay. The AChE activity was determined according to the method of Ellman *et al.*[15] The assay consists of 4 mM potassium phosphate buffer pH 8.0, 10^{-10} M AChE, 1.25–600 μM enzymatic substrate acetylthiocholine (AcSCh) and 0.67–71.2 μM PyDMA. PyDMA was pre-dissolved in dimethylformamide and added to the assay mixture as 0.1% (v/v). The reaction was monitored by the change of the absorbance at 412 nm in a Cary 5E (VARIAN) spectrometer with a detector counting frequency of 30 Hz and an accumulation time of *ca.* 60 s. The experiments were carried out at 25 °C. The concentrations of the product, from which the kinetic constants of the enzyme are derived, are calculated on the basis of the extinction coefficient of the DTNB-derived anion 5-thio-2-nitrobenzoic acid (14 150 M^{-1} cm^{-1}).[16]

Fluorescence spectra. The fluorescence spectra were measured with a Fluorolog 3–22 (Jobin Yvon-Spex). The emission spectra were taken in 0.5 nm steps at a fixed excitation wavelength of 337 nm. The slits were adjusted to 1 nm bandwidth for both excitation and emission. The recorded spectra were automatically corrected for the wavelength dependence of the lamp intensity, monochromator transmission and photomultiplier response. For the experiments in aqueous solution, 10^{-5} M PyDMA was dissolved in DMF and 0.5% (v/v) of this solution was added to the buffer without enzyme. The sensor activity of PyDMA was measured with a solution containing 44.5 nM PyDMA, 0.5% (v/v) DMF and 11.2 μM AChE in the buffer.

Refraction index. A Carl Zeiss refractometer with controlled temperature settings (20 °C) was used to measure the refraction index of the buffer solution containing 44.5 nM PyDMA, 0.5% (v/v) DMF and 11.2 μM AChE.

Computational treatment. The data were treated using the software package ORIGIN 7.0. The software Swiss PDB viewer,[17] Rasmol 2.0[18] and Hyperchem were used for structure visualization and representation of the protein.[19,20]

Results and discussion

Investigations on the microenvironmental dielectric properties of AChE

Lippert–Mataga plot. The concept developed in this article is based on the observation that the spectral response of a chemical system such as *N*,*N*-dimethyl(4-pyren-1-ylphenyl)amine (PyDMA) dissolved in different solvents strongly depends on the dielectric properties of its environment.[14,22] As sketched in Fig. 1 an electron is transferred from the electron donor *N*,*N*-dimethylamino group to the electron acceptor pyrene during or shortly after optical excitation in PyDMA, leading to the formation of an intramolecular charge transfer (ICT) state. The ICT state is characterized by a high dipole moment of about 20 Debye to which the solvent surrounding reacts with reorganization. The stabilization of the transient CT state depends on the dielectric properties of the solvent and leads to a solvent-dependent bathochromic shift of the CT fluorescence spectra. The red-shift of the fluorescence spectra increases with increasing dielectric constant. In the scheme, the solvation of the ICT state is presented by the solvation coordinate σ. Actually, the bathochromic shift of the PyDMA fluorescence is visible by eye, depending on the dielectric properties of the solvent used to dilute PyDMA. In solvents with low dielectric constant, the fluorescence of the sample with daylight is blue, and as the dielectric constant increases with changing solvent, the colour of the fluorescence can be tuned from blue *via* yellow and green to red.

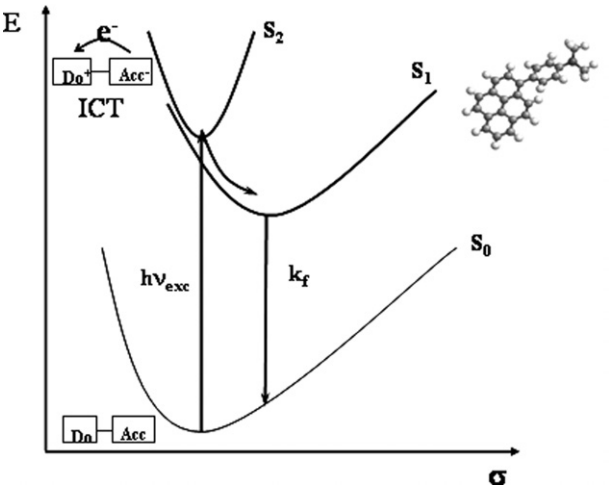

Fig. 1 Photophysical reaction scheme of *N*,*N*-dimethyl(4-pyren-1-ylphenyl)amine (PyDMA) for different solvents; σ is the solvation coordinate. Inset: Structure of PyDMA.

Mathematically, this proportionality is described by the so-called Lippert–Mataga plot, where the gradient of the CT emission band maximum $\tilde{\nu}_{max}$ with respect to the solvent factor $F = f(\varepsilon_s, n) - 0.5f'(\varepsilon_s, n)$ is proportional to the dipole factor μ^2/ρ^3 by

$$\tilde{\nu}_{max} = \tilde{\nu}^0_{max} - \frac{2\mu^2}{hc\rho^3}\left[f(\varepsilon_s, n) - \frac{1}{2}f'(\varepsilon_s, n)\right]. \qquad (1)$$

Here, $\tilde{\nu}^0_{max}$ is the emission band maximum for zero solvent factor, μ is the dipole moment of the fluorescing species and ρ is the radius of the molecule, h is Planck's constant, c is the speed of light in a medium, ε_s is the dielectric constant of the solution and n is its refraction index.

Using the spherical approach for the shape of PyDMA molecules the following solvent factor might be used:

$$F = f(\varepsilon_s, n) - \frac{1}{2}f'(\varepsilon_s, n) = \frac{\varepsilon_s - 1}{\varepsilon_s + 2} - \frac{n^2 - 1}{2n^2 + 1}. \qquad (2)$$

The Lippert–Mataga plot is used generally to estimate the dipole moment of a fluorescing CT species. Fig. 2 presents the Lippert–Mataga plot of PyDMA derived for solvents with a dielectric constant ranging from $\varepsilon_s = 1.4$ (*n*-hexane) to $\varepsilon_s = 78.3$ (0.5% (v/v) DMF–water mixture). For the calculation of the solvent factor, the dielectric constants and refraction indices of the several solvents were taken from ref. 21.

Taking the gradient of the line plot, for PyDMA a dipole moment of μ_{CT} (PyDMA) = 21–22 D (±5 D) is calculated if one assumes a molecular volume $V_{mol} = \rho^3_{molec} \approx 7^3$–$9^3$ Å^3.[14,22]

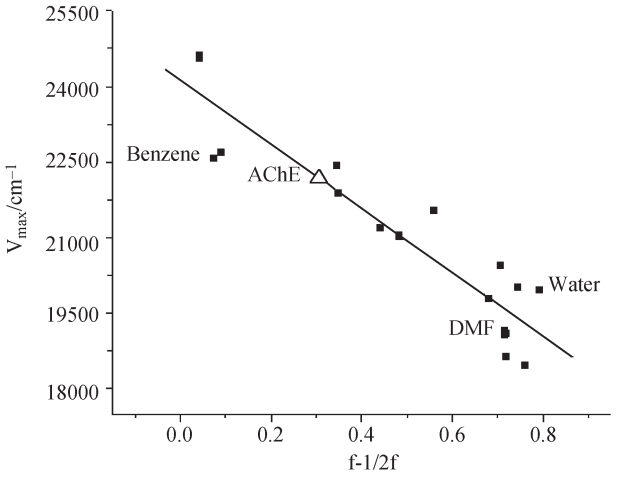

Fig. 2 Lippert–Mataga plot for PyDMA in several solvents (■). The aqueous solutions contain 0.5% (v/v) DMF. The $F = f - 1/2f'$ parameter of the solution with AChE–PyDMA complexes (averaged ratio of the complex = 252:1) was calculated from the linear fit (△).

Note, that the scatter of the experimental values around the Lippert–Mataga plot (eqn. (2)) results from both the error bar of the experimental values and the limitations concerning the models to calculate the molecular volume of PyDMA. Both influences have been intensively discussed in refs. 14 and 22.

In this work, we use a reversed procedure and apply the known Lippert–Mataga plot of PyDMA to the elucidation of the unknown microenvironmental dielectric properties of the binding site(s) of AChE with PyDMA by measuring the red-shift of the PyDMA fluorescence. PyDMA is an ideal candidate for such a detection scheme, first, because of the high transient dipole moment and, second, because of its high fluorescence quantum yield of about unity, independent of the solvent. Thus, one can state that, within the errors of the applied approximations, models and measurements, PyDMA is a suitable sensor for monitoring the microenvironmental dielectric properties of AChE, with the known Lippert–Mataga plot as the calibration curve.

Dielectric properties of the active site of AChE. Fig. 3 summarises the red-shift of the PyDMA fluorescence in different solvents and in aqueous solution in the presence of AChE.

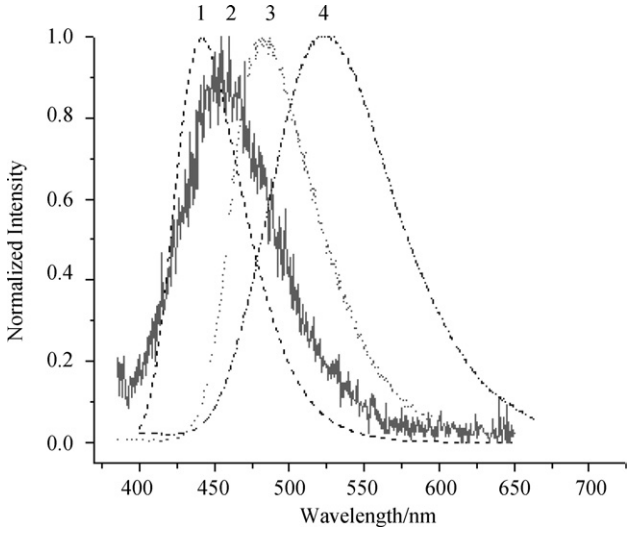

Fig. 3 Fluorescence emission spectra of PyDMA in different solvents. (1) 10^{-5} M PyDMA in benzene; (2) 44.5 nM PyDMA, 11.2 μM AChE in a 0.5% (v/v) DMF–water mixture; (3) 25 μM PyDMA in 0.5% (v/v) DMF–water; (4) 10^{-5} M PyDMA in DMF.

In pure benzene, PyDMA fluoresces at 442.5 nm (22 560 cm^{-1}) (spectrum 1). The PyDMA fluorescence in buffer solution and in the presence of 11.2 μM AChE in an H_2O–0.5% (v/v) DMF mixture is *ca.* 20 nm red-shifted (450 nm, 22 176 cm^{-1}) (spectrum 2) while the PyDMA emission maximum is at 483.5 nm (19 960 cm^{-1}) in an H_2O–0.5% (v/v) DMF mixture (spectrum 3) and at 523.5 nm (19 130 cm^{-1}) in absolute DMF (spectrum 4). The present bathochromic shift shows that the fluorescence of PyDMA attached to AChE does not reflect the dielectric properties of water or DMF–water mixtures, but surprisingly those of benzene or toluene which are aromatic-containing solvents.

The spectral data were quantitatively evaluated by fitting the profile of the fluorescence band with a log–normal function as defined in ref. 14. The linear regression of the Lippert–Mataga plot (see Fig. 2) results in $y = A + Bx$ with the fitting parameters $A = 24\,110 \pm 360$ $cm^{-1}$and $B = -6360 \pm 630$ cm^{-1}. Note that according to eqn. (1) A and B are defined as $A = \tilde{\nu}^0_{max}$ and $B = 2\mu^2/hc\rho^3$. For $y = 22\,176$ cm^{-1}, as found for the PyDMA–AChE system, a solvent constant of $F = 0.30491$ was found. Substituting in eqn. (2), with a measured refraction index of $n = 1.3331$ and hence $(n^2 - 1)/(2n^2 + 1) = 0.170642$, a microenvironmental dielectric constant of $\varepsilon_s = 3.72$ has been found which is slightly higher than the dielectric constant of toluene ($\varepsilon_s = 2.38$), but far away from that of DMF–water mixtures ($\varepsilon_s = 78.3$).

Two approximations mainly limit the presented method: first, in the used model the molecule is treated as a point dipole in the center with no three-dimensional expansions. It is possible to describe the charge distribution in PyDMA more realistically by correcting the data for a cigar-shaped dipole. However, using this model does not improve the dipole moment error dramatically. Here, it should be pointed out that eqn. (1) originally was derived for sandwich-like donor–acceptor complexes and therefore all corrections on the shape will not improve the dipole moment determination by orders of magnitude. Second, the method of dipole moment determination is based on the classical treatment of the solvent as a dielectric continuum. Thus, the determination of the dielectric constant from the Lippert–Mataga plot will always give a microenvironmental dielectric constant which is an average over a sum of unknown local dielectric constants. However, it is possible to treat a microenvironment around a PyDMA dye in a dielectric continuum model. This has been successfully applied to the studies on the microstructure of preferential solvation by these kinds of pyrene dyes.[23]

Analysis of the enzymatic reaction: competitive inhibition of AChE by PyDMA

Data analysis. The interaction of an enzyme E with its substrate S and a competitive inhibitor I can be described as

$$\begin{array}{l} \mathrm{E} + \mathrm{S} \underset{k_1}{\overset{k_{-1}}{\rightleftharpoons}} \mathrm{ES} \xrightarrow{k_2} \mathrm{P} \\ + \\ \mathrm{I} \\ \downarrow\uparrow K_\mathrm{i} \\ EI \end{array} \qquad (3)$$

where k_1 is the rate constant of the enzyme–substrate complex formation, k_{-1} is the rate constant of the enzyme–substrate complex decomposition, k_2 is the catalytic rate constant and K_i is the inhibition constant, which is an equilibrium constant. In our system, E is AChE, S is AcSCh, ES is the enzyme–substrate complex and I is the inhibitor PyDMA, which acts simultaneously as a microenvironmental sensor. Taking into account the steady-state approach $d[ES]/dt = 0$, the rate constants of the enzymatic reaction were calculated according to the Michaelis–Menten equation.

The inhibition reaction of the enzyme can be characterized as competitive, non-competitive or uncompetitive by analysing the Lineweaver–Burk plot.[24] In the present work, competitive inhibition was found (Fig. 4) with a reaction rate of[24]

$$V = \frac{V_{max}[S]}{K_m\left(1 + \frac{[I]}{K_i}\right) + [S]} \quad (4)$$

Here V is the observed rate of reaction, V_{max} is the maximal rate of reaction and [S] is the substrate concentration. [I] is the inhibitor concentration, K_i the inhibition constant and $K_m = (k_2 + k_{-1})/k_1$ the Michaelis–Menten constant.

In the Lineweaver–Burk plot in Fig. 4 the maximal rate constant V_{max} is kept constant whereas the Michaelis constant K_m increases. Since a competitive inhibitor is defined as an inhibitor which combines with the free enzyme in such a way that substrate binding is prevented, *i.e.*, the inhibitor and the substrate are mutually exclusive, the results of Fig. 4 lead to the conclusion that PyDMA combines with free AChE in such a way, that substrate binding is prevented.

The inhibition constant K_i can be determined from the dependence of the Michaelis constant K'_m for increasing inhibitor concentration *versus* the inhibitor concentration [I]:

$$K_m' = K_m + \frac{K_m}{K_i}[I] \quad (5)$$

Here, K_m is the Michaelis constant in the absence of the inhibitor, and the x-intercept corresponds to $-K_i$.[24]

The results from treating the data according to eqn. (5) are summarized in Fig. 5. An inhibition constant of $K_i = 50.97$ μM was found.

Location of PyDMA in the active site of AChE. The finding that PyDMA, a sensor which is sensitive to the dielectric properties of the microenvironment, acts as a competitive inhibitor suggests that PyDMA docks at the active site of AChE or in the gorge. This finding is consistent with studies on other inhibitor systems with dimethyl or trimethylamino groups, which were found to be able to interact with the active site of the anionic subsite. In comparison to the natural substrate acetylcholine, compounds with quaternary ammonium, *e.g.* acethylthiocholine and acethylselenocholine, have an increased relative catalytic efficiency of 1.58 and 3.56, while in compounds with trimethylamino-like *N*,*N*-dimethylaminoethyl acetate a decreased efficiency of 0.076 was found.

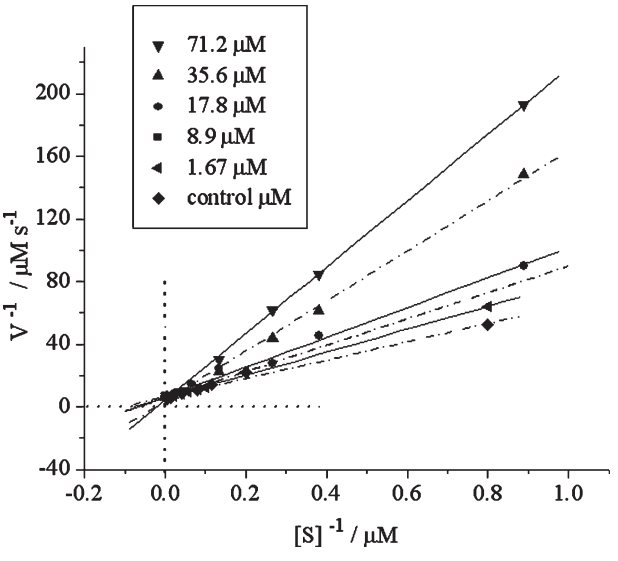

Fig. 4 Competitive inhibition of AChE by PyDMA shown in the Lineweaver–Burk plot; V represents the rate of the enzymatic reaction. The different inhibitor concentrations are in μM.

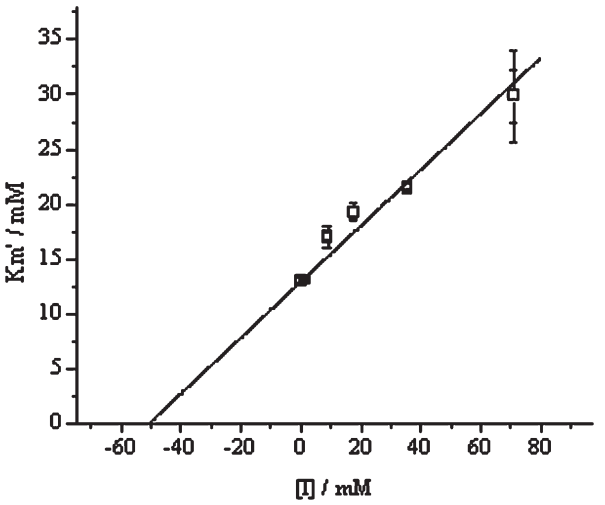

Fig. 5 Plot of apparent K_m ($= K'_m$) *versus* PyDMA concentration [I]. The x-axis intercept corresponds to $-K_i$, so that $K_i = 50.97$ μM.

Methylamino- and amino-containing substrates as *N*-methylaminoethyl acetate and aminoethyl acetate have a relative catalytic efficiency of 3×10^{-3} and 1.6×10^{-4}.[25] With increasing number of methyl substitutions on the nitrogen, steric effects play an important role and the activity increases by orders of magnitude. Crystal structures of AChE with inhibitors also suggest that the amino groups favour to dock on the anionic subsite of the active site, where they can interact.[26,27]

Based on these data we propose that the *N*,*N*-dimethylamino group of PyDMA also attaches to the anionic site. In this position the apolar and aromatic pyrene is able to interact with the aromatic moieties of the AChE gorge, additionally stabilizing the inhibitor–enzyme complex. This orientation of PyDMA in the AChE gorge would also explain the found microenvironmental dielectric constant of AChE which is similar to that of aromatic solvents like toluene or benzene.

This hypothesis is also supported by computer simulations based on an AMBER forcefield optimization.[19,20] For the simulations, the amino acids of the active site were kept rigid in a surrounding continuum and PyDMA was attached to and in the hole of the active site. For the energy minimization, the whole molecule PyDMA was rotated in the hole of the active site and a convergence of the energy minimization was found only for the configuration shown in Fig. 6(b). Similar to the systems described above, this configuration allows the *N*,*N*-dimethylamino moiety of PyDMA to interact with the anionic site and the pyrene group with the aromatic residues of the gorge (Fig. 6(b) and (c)). The distance between the pyrene group and the closest amino acid of the gorge, Phe 338, is about 3.70 Å (Fig. 6(d)). Excimer formation, which would quench the fluorescence of PyDMA, has not yet been explicitly investigated and will be a topic of future studies.

Conclusion

The laser dye *N*,*N*-dimethyl(4-pyrene-1-ylphenyl)amine (PyDMA) can be used to detect the permittivity of the microenvironment of the binding site in the active site of AChE enzyme. The determination of microenvironmental dielectric properties by the quantitative treatment of the bathochromic shift of the PyDMA fluorescence spectra according to the Lippert–Mataga plot was applied. The analysis of the kinetics of the enzyme showed a competitive inhibition of the activity in the presence of PyDMA.

Both the results obtained by spectroscopy and the results obtained by kinetic analysis support the structure model,

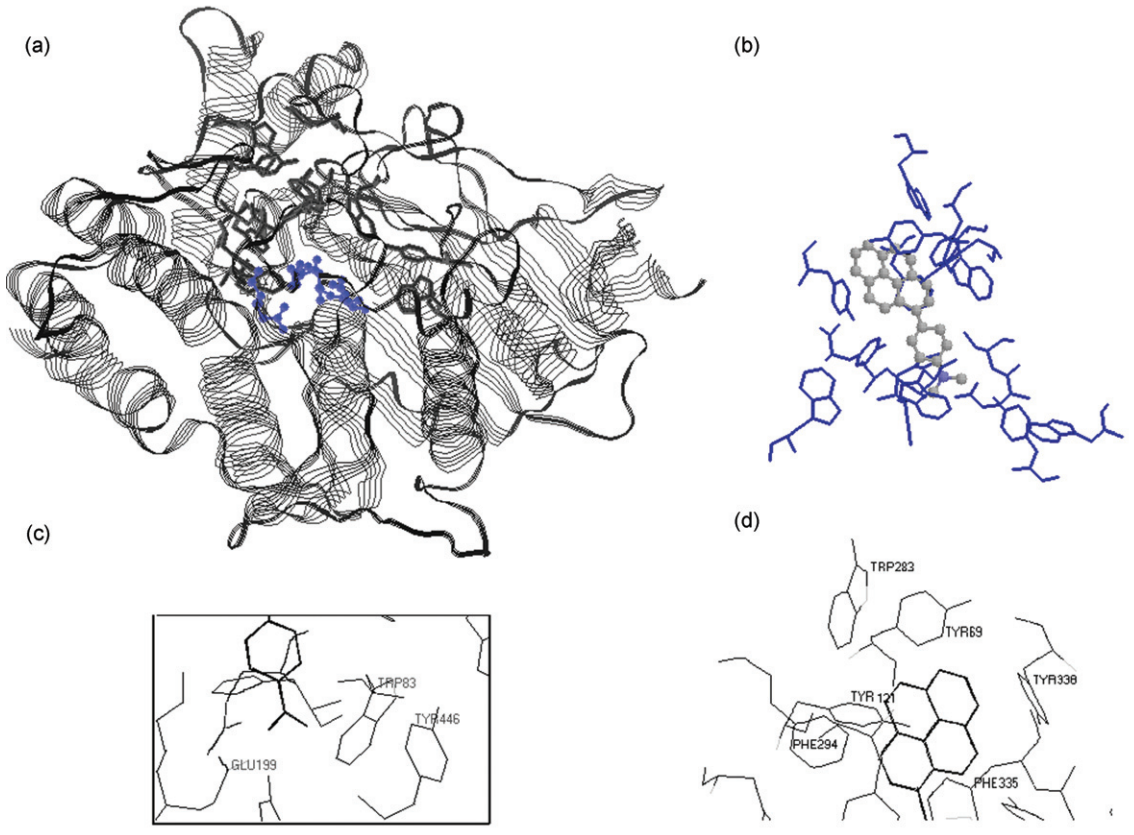

Fig. 6 Structure of acetylcholinesterase, free and complexed with the sensor and competitive inhibitor PyDMA: (a) AChE structure according to the crystal structure in ref. 28, with the amino acids of the gorge by a stick representation and the active site (esteratic subsite) in blue by ball and stick representation; (b) AChE gorge structure complexed with PyDMA, the active site and gorge are presented by sticks and PyDMA by ball and stick representation; (c) interaction of the *N*,*N*-dimethylamino group of PyDMA and the amino acids of the anionic site; (d) interaction of the pyrene group of PyDMA with the aromatic residues of the gorge.

where PyDMA is located in the active site oriented in such a way that the pyrene moiety can interact with the aromatic residues of the gorge and the amino moiety points to the anionic subsite. These findings are also supported by force-field calculations of the PyDMA–AChE complex.

Based on the present work we suggest that PyDMA, or laser dyes with similar spectroscopic properties and chemical components, has the potential to be developed as a biosensing element for dielectric properties of AChE enzyme or enzymes with similar substrate specificity.

Acknowledgements

A. R. thanks the DAAD (PKZ: A/01/16759) and S. T. is grateful to DFG for support (TE 347/1-1). I. Dreger is thanked for technical assistance and J. Troe for permanent support of the work.

References

1 J. Heemskerk, A. J. Tobin and L. J. Bain, *Trends Neurosci.*, 2002, **25**, 494–496.
2 N. J. Tillakaratne, R. D. de Leon, T. X. Hoang, R. R. Roy, V. R. Edgerton and A. J. Tobin, *J. Neurosci.*, 2002, **22**, 3130–3143.
3 M. Keusgen, *Naturwissenschaften*, 2002, **89**, 433–444.
4 J. E. Gestwicki, H. V. Hsieh and J. B. Pitner, *Anal. Chem.*, 2001, **73**, 5732–5737.
5 E. Topoglidis, T. Lutz, R. L. Willis, C. J. Barnett, A. E. G. Cass and J. A. Durrant, *Faraday Discuss.*, 2000, **116**, 35.
6 E. Topoglidis, A. E. G. Cass, G. Gilardi, S. Sadeghi, N. Bourmont and J. A. Durrant, *Anal. Chem.*, 1998, **70**, 5111.
7 D. C. Cowell, A. K. Abass, A. A. Dowman, J. P. Hart, R. M. Pemberton and S. J. Young, in *Biomonitors and Biomarkers as Indicators for Environmental Change, Vol. II*, ed. F. M. Butterworth, A. Gunatilika and M. E. Gonsebatt, Kluwer Academic/Plenum Publishing Corp., New York, 2000, pp. 157–174.
8 J. L. Sussman, M. Harel, F. Frolow, C. Oefner, A. Goldman, L. Toker and I. Silman, *Science*, 1991, **253**, 872–879.
9 A. Shafferman, C. Kronman, Y. Flashner, M. Leitner, H. Grosfeld, A. Ordentlich, Y. Gozes, S. Cohen, N. Ariel and D. Barak, *J. Biol. Chem.*, 1992, **267**, 17 640–17 648.
10 P. Taylor, in *The Pharmacological Basis of Therapeutics*, ed. A. G. Gilman, T. W. Rall, A. Nies and P. Taylor, Pergamon, New York, 1990, pp. 131–149.
11 E. J. Barreiro, C. A. Camara, H. Verli, L. Brazil-Mas, N. G. Castro, W. M. Cintra, Y. Aracava, C. R. Rodrigues and C. A. Fraga, *J. Med. Chem.*, 2003, **46**, 1144–1152.
12 T. Simonson, *Curr. Opin. Struct. Biol.*, 2001, **11**, 243–252.
13 F. Li and Z. Han, *Arch. Inst. Biochem. Physiol.*, 2002, **51**, 37–45.
14 S. Techert, S. Schmatz, A. Wiessner and H. Staerk, *J. Phys. Chem. B*, 2000, **105**, 7579–7587.
15 G. L. Ellman, D. Courtey, V. Andres and R. M. Featherstone, *Biochem. Pharmaceut.*, 1961, **7**, 88–95.
16 P. W. Riddles, R. L. Blakeley and B. Zerner, *Anal. Biochem.*, 1979, **94**, 75–81.
17 http://us.expasy.org/spdbv/.
18 http://www.bernstein-plus-sons.com/software/rasmol/.
19 R. Fletcher, *Pratical Methods of Optimization*, John Wiley & Sons, New York, 1980.
20 Hyperchem®, *Computational Chemistry: Molecular Visualization and Simulation*, Hypercube, Inc., Ontario, 1994.
21 D. R. Lide, *CRC Handbook of Chemistry and Physics*, CRC Press, Cleveland, OH, 84th edn., 2003.
22 S. Techert, S. Schmatz, A. Wiessner and H. Staerk, *J. Phys. Chem. A*, 2000, **104**, 5700–5712.
23 N. Kh. Petrov, A. Wiessner and H. Staerk, *J. Chem. Phys.*, 1998, **108**, 2326.
24 I. H. Segel, *Biochemical Calculations*, John Wiley & Sons, Inc., New York, 1976.

25 D. M. Quin, *Chem. Rev.*, 1987, **87**, 955–979.
26 H. Dvir, D. M. Wong, M. Harel, X. Barril, M. Orozco, F. J. Luque, D. Munoz-Torrero, P. Camps, T. L. Rosenberry, I. Silman and J. L. Sussman, *Biochemistry*, 2002, **41**, 2970–2981.
27 M. Harel, D. M. Quinn, H. K. Nair, I. Silman and J. L. Sussman, *J. Am. Chem. Soc.*, 1996, **118**, 2340–2346.
28 Y. Bourne, J. Grassi, P. E. Bougis and P. Marchot, *J. Biol. Chem.*, 1999, **274**, 30 370–30 376.